Nonlinear Optics

DOI: 10.1002/anie.201103691

Strongly Nonlinear Optical Chalcogenide Thin Films of $APSe_6$ (A=K, Rb) from Spin-Coating**

*In Chung, Myung-Gil Kim, Joon I. Jang, Jiaqing He, John B. Ketterson, and Mercouri G. Kanatzidis**

Second-order nonlinear optical (NLO) effects[1] in the infrared region allow for all-optical high-capacity communication networks,[2] tunable mid-infrared light sources that are hard to reach by other means, remote sensing,[3–6] and medical diagnostics.[7–9] The key to these applications is the availability of an appropriate NLO medium. However, obtaining NLO inorganic crystals and films involves high-cost and lengthy processes. To date, chalcogenide films for IR applications with high conversion efficiencies have been lacking. Herein we present the first example of a solution-based deposition process of strongly nonlinear optical inorganic thin films deposited on silicon, glass, and flexible plastic substrates at low temperatures of 125–250 °C. The obtained glassy and crystalline films of highly nonlinear $APSe_6$ compounds (A = K, Rb; $\chi^{(2)} \approx 150\ \mathrm{pm\,V^{-1}}$)[10,11] exhibited strong, inherent second harmonic and difference frequency generation (SHG and DFG) in the visible and near IR spectral region at room temperature without the need of poling.

Second-order nonlinear optical (NLO) phenomena are effective at producing a coherent beam of tunable light frequencies that access regions, in which lasers perform poorly or are unavailable.[12] Although technologies for tunable lasers have been developed over decades, commercially available wavelength ranges with reasonable efficiency are still severely limited.[13] An NLO medium such as some inorganic crystals enables two incoming light waves of frequency ω_1 and ω_2 to interact, thus producing four different frequencies: $2\omega_1$ and $2\omega_2$ by second harmonic generation (SHG) and mixed frequencies $|\omega_1 \pm \omega_2|$ by difference and sum frequency generation (DFG and SFG).[1] The region of the spectrum between 2–12 μm is in high demand for tunable and coherent IR laser sources, because it is useful in several important applications.[14] These include remote sensing organic and inorganic molecules for homeland security and environmental monitoring applications (including biohazards,[3] explosives,[5] chemical warfare agents,[6] and pollutants[4]) as well as in minimally invasive medical surgery;[7] direct imaging of anisotropic biological structures in tissues, cell metabolism, and disease states such as Alzeheimer's disease and cancer.[9] These applications favor portable instruments that require a high-performing, lightweight, shock-tolerable, and inexpensive (sometimes disposable and easily replaceable) NLO medium. Indeed, a main challenge for these NLO applications is the costly, lengthy, and labor-intensive processes to synthesize sizable, optical quality inorganic NLO single crystals. On the other hand, thin films of organic/polymer NLO materials are solution-processable but are far from practical applications because of issues of thermal stability, low-laser damage threshold, and critical light absorption that prohibits essential DFG performance in most of the IR region.[15]

Previously, we have shown that amorphous glassy forms of noncentrosymmetric phase-change materials can retain memory of the crystal structure to be overall noncentrosymmetric themselves.[16] A remarkable example is the case of the selenophosphate compounds $APSe_6$ (A = K, Rb) (Figure 1a). They are one-dimensional inorganic polymers with anionic chains of $^1_\infty[PSe_6^{-1}]$ (Figure 1b) separated by A^+ cations. These phase change materials possess record-high SHG coefficients $\chi^{(2)}$ of 151.3 $\mathrm{pm\,V^{-1}}$ and 149.4 $\mathrm{pm\,V^{-1}}$ for K^+ and Rb^+ salts, respectively, among phase-matchable NLO materials with a band gap over 1.0 eV.[10–11] In their glass state, these compounds are an exception to the general rule that

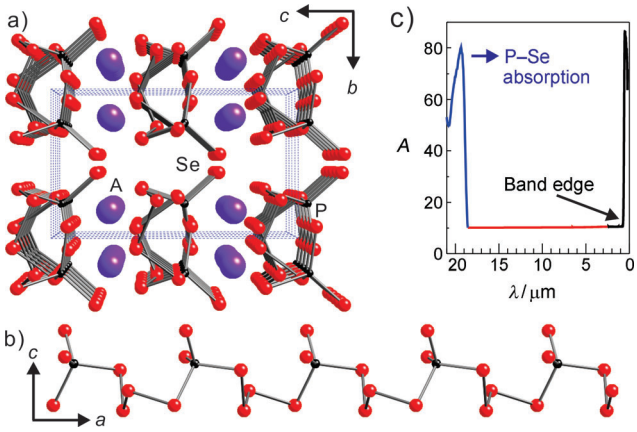

Figure 1. Crystal structure of $APSe_6$. a) Unit cell viewed down the crystallographic *a* axis parallel to the chain propagating direction, showing the polar nature of the structure. A: blue, P: black, Se: red. b) View of a polymeric chain of $^1_\infty[PSe_6^{-1}]$. c) Far-IR (blue line)/mid-IR (red)/visible (black) absorption spectra of $KPSe_6$ glass showing wide transparency range.

[*] Dr. I. Chung, M. Kim, Dr. J. He, Prof. M. G. Kanatzidis
Department of Chemistry, Northwestern University
2145 Sheridan Rd., Evanston, IL 60208 (USA)
E-mail: m-kanatzidis@northwestern.edu
Homepage: http://chemgroups.northwestern.edu/kanatzidis/
Dr. J. I. Jang, Prof. J. B. Ketterson
Department of Physics and Astronomy, Northwestern University
2145 Sheridan Rd., Evanston, IL 60208 (USA)

[**] Financial support was provided by the National Science Foundation (Grant DMR-1104965).

Supporting information for this article is available on the WWW under http://dx.doi.org/10.1002/anie.201103691.

required amorphous states lack second-order optical nonlinearity due to the presence of a center of symmetry on a macroscopic level. In contrast, the amorphous $APSe_6$ remarkably exhibit comparable SHG intensities to a benchmark IR NLO material $AgGaSe_2$[17] without any poling.[10,18] Both compounds melt congruently and can be grown into long glass fibers that can perform wave-guiding operations and show strong NLO effects. These materials are widely transparent in the visible and IR region of the spectrum (Figure 1c) and are soluble in polar solvents.

Herein we demonstrate that the $APSe_6$ can be solution-processed into smooth amorphous thin films with strong and permanent NLO response using low-cost methods previously developed for conjugated organic polymers,[19] electronic oxides,[20] and chalcogenides.[21] The amorphous films can then be readily switched to crystalline films by heating, thus achieving an even greater boost in NLO efficiency. The inorganic NLO thin films we describe here are the first example of solution-based spin-coat deposited systems capable of operating in the IR.

The fabrication of films of $APSe_6$ is straightforward and is illustrated in Figure 2. $APSe_6$ powders were dissolved in anhydrous *N*,*N*-dimethylformamide (DMF) or N_2H_4 to give viscous solutions. The resulting solutions were diluted to various concentrations and spin-coated on Si, glass, and flexible plastic (AryLite) substrates at a rate of 1000 rpm for 40 s, followed by drying at 125 °C for 5 min to give transparent orange glassy thin films. The film thickness is controllable by changing the concentration of the $APSe_6$ solutions and spinning rates. The films on the flexible plastic substrates were intact with no cracks when bent (Figure 3a), lightweight, and shock-tolerable. The glassy thin films can be converted to highly crystalline films with no cracks or peeling after annealing above the crystallization point at 220–250 °C for 5–10 min.

Atomic force microscopy (AFM) images of a typical $RbPSe_6$ glassy film (thickness ca. 100 nm) show excellent surface smoothness with a root-mean-squared (r.m.s.) roughness less than 1 nm (Figure 3b). Scanning electron microscopy (SEM) images of glass $RbPSe_6$ films showed a smooth and continuous surface and well-defined edges (Figure 3c). Energy-dispersive spectroscopy confirms the compositions of $KPSe_6$ and $RbPSe_6$. In contrast, films of chalcogenide compounds deposited by thermal evaporation and e-beam irradiation generally suffer from rough surfaces, significant defects and poor control of chemical composition. The cross-sectional TEM image of the glassy film showed amorphous morphology with no evidence of crystalline nanoparticles embedded in the film. The electron diffraction pattern taken from the same area gave faint, diffuse rings, thus confirming the amorphous nature of the nanoparticles (Figure 3d). These results rule out the presence of any crystalline nanoparticles in the amorphous films. The strong diffraction peaks observed stem from the Si substrate. Furthermore, the X-ray diffraction pattern of the thin film gave no Bragg peaks, thus supporting the results of the TEM studies (Figure 3e).

The as-deposited glassy $APSe_6$ thin films rapidly convert to crystalline ones when heated at 220–250 °C for 5 min as expected for a phase-change material. The crystallized films are transparent light orange in color with no pealing evident after heat treatment. The X-ray diffraction pattern of the $RbPSe_6$ thin film is consistent with the theoretically calculated one based on the single-crystal structure (Figure 3e). The narrow peak width of the Bragg peaks confirms the high crystallinity.

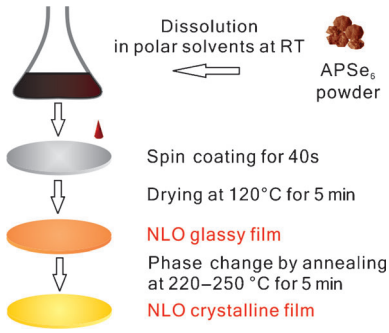

Figure 2. Schematic illustration of $APSe_6$ thin film fabrication procedure.

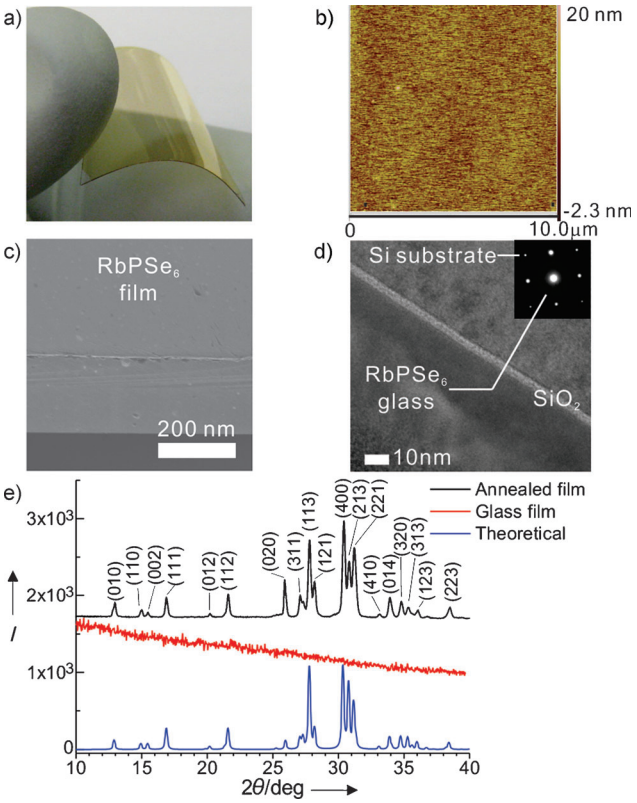

Figure 3. a) A photograph of $RbPSe_6$ optical glassy thin film on the flexible plastic (AryLite) substrate. b) AFM image of $RbPSe_6$ glassy thin film (100 nm thick). The panel shows 10 μm × 10 μm scan with an r.m.s. roughness less than 1 nm, representing surface smoothness and uniformity. c) Representative SEM image of $RbPSe_6$ film, showing a smooth surface. d) Cross-sectional TEM image of $RbPSe_6$ glass thin film on a Si substrate. The electron-diffraction pattern on the area (inset) showed faint diffuse rings confirming the amorphous nature of the film. The strong diffraction signals result from the Si substrate. e) Grazing incident angle thin film X-ray diffraction patterns of glassy and crystallized $RbPSe_6$ films and theoretical calculations for comparison. The (*hkl*) index on the major signals is presented.

We examined as-prepared amorphous thin films (ca. 100 nm thickness) of $APSe_6$ (A = K, Rb) for SHG NLO response. Incident light pulses of 10 μJ were generated by an optical parametric amplifier (OPA) driven by a pulsed Nd:YAG laser (30 ps) at 355 nm with a repetition rate of 10 Hz. Aligning the thin films (1.25 cm × 1.25 cm × 100 nm) parallel to the laser path, we focused the idler beam (λ_2 = 1000–1800 nm) from the OPA on the proximal edge of the film, and the wave-guided outgoing light was collected from the distal edge of the film (Figure 4a). We observed that as-prepared $APSe_6$ (A = K, Rb) glass films act as frequency converters in wave-guided mode to produce doubled frequencies over a wide spectral range from visible to near IR (Figure 4b). Note that frequency-doubled light travelled through a macroscopic length of 1.25 cm of amorphous film. This observation is the first example of optical amorphous films exhibiting innate, strong SHG responses without the need of poling. It should be noted that previously investigated artificially poled glasses of GeO_2–SiO_2 with induced SHG exhibited only weak signals and were temporally unstable at room temperature.[22]

Remarkably, the crystalline films derived from the amorphous films exhibited approximately 30 times stronger SHG intensities in wave-guided mode. Because DFG is a core property to produce mid-IR light[23] and necessary to facilitate multichannel conversion and all-optical networks,[2] we carried out DFG experiments. By introducing the combination of two incident beams (wavelengths ω_1 and ω_2), the $RbPSe_6$ crystalline film nonlinearly mixed frequencies to generate continuously tunable near-IR light by DFG (Figure 4c). For example, a new light beam at 818 nm was obtained by mixing two distinct light waves with wavelengths at 495 nm and 1254 nm as defined by DFG:

$$\lambda_{DFG} = \left(\frac{\lambda_{idler}}{\lambda_{idler} - 710}\right) 355\text{nm} \quad (1)$$

Although our current experimental detection limit (< 1 μm) prohibited observing DFG in the mid-IR, $APSe_6$ (A = K, Rb) should also produce tunable coherent light throughout the mid-IR region because the compounds are optically transparent up to 19–20 μm (Figure 1c),[10] a region in which few suitable NLO materials are available.[23] Figure 3d and Supporting Movie S1 clearly demonstrate the capability of a $RbPSe_6$ crystalline film to act as a frequency doubler: generating very strong SHG visible lights from green to orange to red from invisible IR incident beams, thereby providing continuous frequency tunability.

Other materials, in which solution processing is important in their utilization include amorphous oxide semiconductors[20] with high-performance in thin film transistors (TFTs) in displays and photovoltaic metal chalcogenides.[24] In these systems, high temperatures are necessary because the processes involve decomposition of solution precursors to dense films, which is accompanied by the creation of volatile byproducts that need to be completely removed. In the present case, the precursor and the final product are the same (i.e., $APSe_6$) and the deposition of the films is facile and can occur at lower temperatures.

We demonstrated the fabrication of $APSe_6$ (A = K, Rb) films on large-area substrates including a flexible plastic. The materials perform NLO processes exceptionally well in the IR region and the fabrication costs, time, and simplicity are superior to any reported methods for NLO thin films. The procedure can be widely applied to many compounds of this class of NLO materials, such as $A_2P_2Se_6$ (A = K, Rb, Cs),[18] AM_5Q_8 (A = K, Rb, Tl; M = Sb, Bi; Q = S, Se),[25] and $AAsQ_2$ (A = Li, Na; Q = S, Se).[26] These results point to a path that circumvents a bottleneck in NLO applications of inorganic IR transparent materials, namely, the preparation of large NLO crystals and thin films using physical deposition methods. Amorphous NLO films on a flexible plastic can open up new opportunities for NLO applications because of the advantages of mechanical flexibility, uniformity, processing temperature, formability, and inexpensive fabrication.

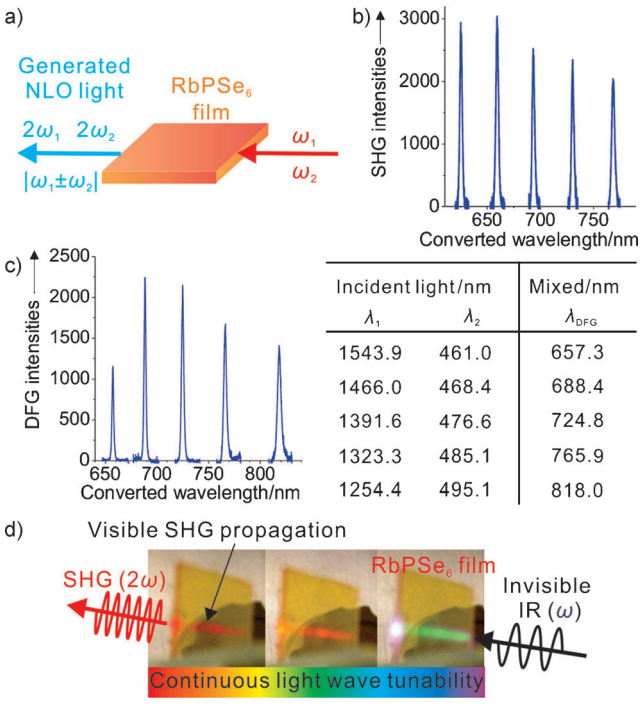

Incident light/nm		Mixed/nm
λ_1	λ_2	λ_{DFG}
1543.9	461.0	657.3
1466.0	468.4	688.4
1391.6	476.6	724.8
1323.3	485.1	765.9
1254.4	495.1	818.0

Figure 4. NLO properties of $RbPSe_6$ optically clear amorphous and crystalline thin films over a wide range of the Vis/near IR region. a) Illustration of NLO property measurements on thin films. b) Wave-guided SHG response transmitted through 1.25 cm × 1.25 cm × 100 nm size of $RbPSe_6$ glassy thin film. c) DFG response of $RbPSe_6$ crystalline film, demonstrating wave-mixing capability over a wide range of wavelengths. Tabulated are the wavelengths of two incident beams and those of nonlinearly mixed DFG lights. d) Photographs of $RbPSe_6$ crystalline film to generate strong visible lights from red to orange to green, by SHG process, representing continuous tunability of light waves.

Experimental Section

Synthesis: Pure amorphous $APSe_6$ (A = K, Rb) materials were prepared by reacting a stoichiometric mixture of A_2Se/P/Se in a 1:2:11 molar ratio under vacuum in a silica tube at 350 °C for 6 h followed by quenching under air. Energy dispersive spectroscopy analysis of the glass ingots showed an average composition of "$KPSe_{5.9}$" and "$RbPSe_{5.9}$", respectively. $KPSe_6$ m.p.: approximately

320 °C, crystallization point: 224 °C; $RbPSe_6$ m.p.: approximately 315 °C, crystallization point: 218 °C.

Thin-film fabrication: Powders of $APSe_6$ glasses (ca. 120–350 mg) were dissolved in polar organic solvents (1.5 mL) of anhydrous *N*,*N*-dimethylformamide (DMF) or N_2H_4 to give viscous solutions. The solutions were filtered through a 0.2 μm syringe filter, and diluted to various concentrations. Amorphous thin films were deposited by a spin-coating process at 1000 rpm for 40 s, followed by drying at 120 °C for 5 min on a hot plate. The complete removal of DMF or N_2H_4 was confirmed by thermal gravimetric analysis (TGA) and mid-IR spectroscopy studies for vacuum-dried bulk powders of $APSe_6$/organic solutions. The amorphous films were converted to crystalline when annealed at 220–250 °C.

Nonlinear optical properties measurements: SHG responses from our films were measured in wave-guided mode as a function of the fundamental wavelength λ_2 (idler beam) from an optical parametric amplifier (OPA), which is synchronously pumped by a frequency-tripled output (355 nm) of a Nd:YAG laser (EKSPLA PL 2143 series). For DFG measurements, we mixed the signal (λ_1) and idler (λ_2) beams from the OPA. The predicted DFG wavelength (λ_{DFG}) is only a function of λ_2 due to twin-photon generation and given by $\lambda_{DFG} = [\lambda_2/(\lambda_2\text{-}710\text{ nm})]355$ nm. The input irradiance was about 200 MW cm^{-2}. The SHG and DFG signals were collected using a fiber-optic bundle and dispersed with a Spex Spec-One 500 M spectrometer coupled to a nitrogen-cooled CCD camera.

Received: May 30, 2011
Revised: August 10, 2011
Published online: September 20, 2011

Keywords: nonlinear optics · phase transitions · selenophosphates · solution processes · thin films

[1] N. Bloembergen, *Nonlinear Optics*, 4th ed., World Scientific, River Edge, NJ, **1996**.
[2] D. Cotter, R. J. Manning, K. J. Blow, A. D. Ellis, A. E. Kelly, D. Nesset, I. D. Phillips, A. J. Poustie, D. C. Rogers, *Science* **1999**, *286*, 1523–1528.
[3] D. Pestov, X. Wang, G. O. Ariunbold, R. K. Murawski, V. A. Sautenkov, A. Dogariu, A. V. Sokolov, M. O. Scully, *Proc. Natl. Acad. Sci. USA* **2008**, *105*, 422–427.
[4] M. Pushkarsky, A. Tsekoun, I. G. Dunayevskiy, R. Go, C. K. N. Patel, *Proc. Natl. Acad. Sci. USA* **2006**, *103*, 10846–10849.
[5] M. B. Pushkarsky, I. G. Dunayevskiy, M. Prasanna, A. G. Tsekoun, R. Go, C. K. N. Patel, *Proc. Natl. Acad. Sci. USA* **2006**, *103*, 19630–19634.
[6] M. B. Pushkarsky, M. E. Webber, T. Macdonald, C. K. N. Patel, *Appl. Phys. Lett.* **2006**, *88*, 044103.
[7] V. A. Serebryakov, E. V. Boiko, N. N. Petrishchev, A. V. Yan, *J. Opt. Technol.* **2010**, *77*, 6–17.
[8] B. Jalali, *Nat. Photonics* **2010**, *4*, 506–508.
[9] a) W. R. Zipfel, R. M. Williams, W. W. Webb, *Nat. Biotechnol.* **2003**, *21*, 1369–1376; b) W. R. Zipfel, R. M. Williams, R. Christie, A. Y. Nikitin, B. T. Hyman, W. W. Webb, *Proc. Natl. Acad. Sci. USA* **2003**, *100*, 7075–7080.
[10] I. Chung, J. I. Jang, C. D. Malliakas, J. B. Ketterson, M. G. Kanatzidis, *J. Am. Chem. Soc.* **2010**, *132*, 384–389.
[11] J.-H. Song, A. J. Freeman, T. K. Bera, I. Chung, M. G. Kanatzidis, *Phys. Rev. B* **2009**, *79*, 245203.
[12] M. M. Fejer, *Phys. Today* **1994**, *47*, 25–32.
[13] F. J. Duarte, *Tunable Laser Optics*, Elsevier Academic Press, New York, **2003**.
[14] B. Jean, T. Bende, *Top. Appl. Phys.* **2003**, *89*, 511–544.
[15] L. R. Dalton, P. A. Sullivan, D. H. Bale, *Chem. Rev.* **2010**, *110*, 25–55.
[16] a) M. Wuttig, N. Yamada, *Nat. Mater.* **2007**, *6*, 824–832; b) A. V. Kolobov, P. Fons, A. I. Frenkel, A. L. Ankudinov, J. Tominaga, T. Uruga, *Nat. Mater.* **2004**, *3*, 703–708.
[17] D. N. Nikogosyan, *Nonlinear optical crystals: a complete survey*, 1st ed., Springer, New York, **2005**.
[18] I. Chung, C. D. Malliakas, J. I. Jang, C. G. Canlas, D. P. Weliky, M. G. Kanatzidis, *J. Am. Chem. Soc.* **2007**, *129*, 14996–15006.
[19] S. Günes, H. Neugebauer, N. S. Sariciftci, *Chem. Rev.* **2007**, *107*, 1324–1338.
[20] K. Nomura, H. Ohta, A. Takagi, T. Kamiya, M. Hirano, H. Hosono, *Nature* **2004**, *432*, 488–492.
[21] D. B. Mitzi, L. L. Kosbar, C. E. Murray, M. Copel, A. Afzali, *Nature* **2004**, *428*, 299–303.
[22] T. Fujiwara, M. Takahashi, A. J. Ikushima, *Electron. Lett.* **1997**, *33*, 980–982.
[23] A. Fiore, V. Berger, E. Rosencher, P. Bravetti, J. Nagle, *Nature* **1998**, *391*, 463–466.
[24] a) K. K. Banger, Y. Yamashita, K. Mori, R. L. Peterson, T. Leedham, J. Rickard, H. Sirringhaus, *Nat. Mater.* **2011**, *10*, 45–50; b) B. N. Pal, B. M. Dhar, K. C. See, H. E. Katz, *Nat. Mater.* **2009**, *8*, 898–903.
[25] a) J. B. Wachter, K. Chrissafis, V. Petkov, C. D. Malliakas, D. Bilc, T. Kyratsi, K. M. Paraskevopoulos, S. D. Mahanti, T. Torbrugge, H. Eckert, M. G. Kanatzidis, *J. Solid State Chem.* **2007**, *180*, 420–431; b) T. Kyratsi, K. Chrissafis, J. Wachter, K. M. Paraskevopoulos, M. G. Kanatzidis, *Adv. Mater.* **2003**, *15*, 1428–1431.
[26] a) T. K. Bera, J.-H. Song, A. J. Freeman, J. I. Jang, J. B. Ketterson, M. G. Kanatzidis, *Angew. Chem.* **2008**, *120*, 7946–7950; *Angew. Chem. Int. Ed.* **2008**, *47*, 7828–7832; b) T. K. Bera, J. I. Jang, J.-H. Song, C. D. Malliakas, A. J. Freeman, J. B. Ketterson, M. G. Kanatzidis, *J. Am. Chem. Soc.* **2010**, *132*, 3484–3495.

